Experimental microwave radiometry of a sonoluminescing bubble

John N. Kordomenos,* Miguel Bernard,† and Bruce Denardo‡
Department of Physics and Astronomy and National Center for Physical Acoustics, University of Mississippi, University, Mississippi 38677
(Received 12 October 1998)

In spite of substantial research in single-bubble sonoluminescence this decade, the electromagnetic emission mechanism is still not sufficiently understood. Current models of the mechanism are based on experimentally measured spectra in the visible and near-visible region. An experimental arrangement used to measure the *microwave* emission is described. For a xenon-doped bubble, which emits the greatest amount of light, no microwave radiation is observed at or above the minimum detectable power of the apparatus, which corresponds to a bubble radiating approximately 1 nW in a 1-GHz bandwidth at 2 GHz. Any theory of single-bubble sonoluminescence when extended to the microwave region must be consistent with this upper limit for the radiation. [S1063-651X(99)05002-3]

PACS number(s): 78.60.Mq, 52.70.Gw, 33.20.Bx, 84.40.−x

Analytical models that have been proposed to account for single-bubble sonoluminescence (SL) include thermal bremsstrahlung [1], thermal blackbody radiation [2], Casimir light [3,4], and collision-induced emission [5]. Each of these theories contains different assumptions about the bubble's temperature, pressure, and ionization. When these theories are fit to an observed spectrum in the visible and near-visible region, substantial differences in the predicted powers are expected far from this region, due to the fundamentally different nature of the theories. To our knowledge, none of these theoretical extensions has been established, and no experiments outside the visible and near-visible region have been reported.

The attenuation of electromagnetic radiation by water [6] permits a small window corresponding to visible and near-visible frequencies to reach a SL detector. Most of the electromagnetic spectrum remains hidden to the experimenter except for frequencies in and below the microwave region 10^9-10^{10} Hz, or for frequencies above 10^{18} Hz. For example, regarding a possible measurement in the infrared region $10^{11}-10^{14}$ Hz, the exponential attenuation coefficient is in the range 10^2-10^4 cm^{-1}. Such strong attenuation would require one to probe the radiation at distances shorter than 100 μm from the bubble, which cannot yet readily be accomplished because placing an object closer than 1 mm from the bubble destroys the bubble's stability. For frequencies higher than visible the attenuation coefficient is still very large with an extinction length on the order of a μm. Even for soft x-ray photon energies of 1 keV (10^{17} Hz), the extinction length is a fraction of a millimeter and thus does not lend itself to measurement. These facts led us to consider an experiment in the microwave part of the spectrum.

Figure 1 shows the exponential attenuation coefficient of water as a function of frequency in the microwave region. The coefficient was computed from a semiempirical formula developed to characterize the frequency dependence of the complex dielectric constant of water [7]. The attenuation for 1 GHz at room temperature is sufficiently small to permit 7% of the radiated microwave power to reach an antenna with a cross section 1 cm^2 at a distance of 1 cm from the bubble. In contrast, at 10 GHz the antenna will receive only 4×10^{-6} of the radiated power.

We experimentally explored the frequency range of 0.7 GHz centered at 2.0 GHz. Because the index of refraction for water is 9.0 at 2.0 GHz [6], the center frequency corresponds to wavelength 1.7 cm in water. The SL cell [Fig. 2(a)] consisted of a rectangular plastic container [8], with inner dimensions 5.3×5.3 cm^2 and height 12.3 cm. The water had a height 9.8 cm, and was directly driven by a shielded ultrasonic horn. The cell rested on a piece of styrofoam so that a nodal pressure boundary condition existed on the bottom as well as the other boundaries [8]. A sonoluminescing bubble was created near a pressure antinode of the (1,1,3) mode, which was resonantly driven at 28 kHz.

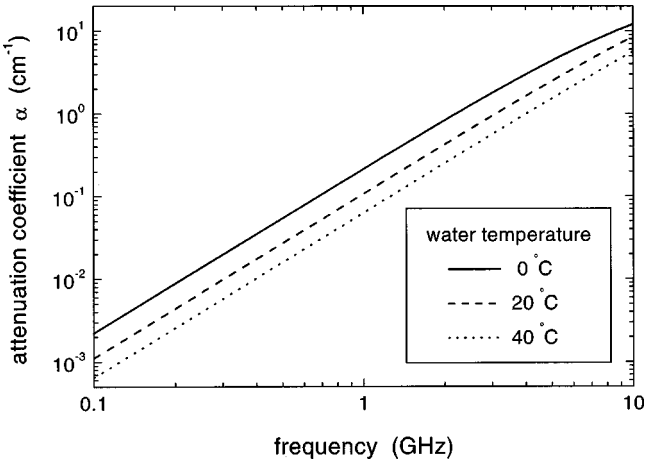

FIG. 1. Attenuation coefficient α of microwave radiation in water as a function of frequency for various temperatures. The intensity of a plane wave attenuates with distance x as $e^{-\alpha x}$.

*Present address: Department of Medical Physics, University of Wisconsin, Madison, Wisconsin 53706. Electronic address: johnk@humonc.wisc.edu

†Present address: McKinsey and Co., 11560 Mexico City, D.F., Mexico.

‡Present address: Physics Department, Naval Postgraduate School, Monterey, CA 93943.

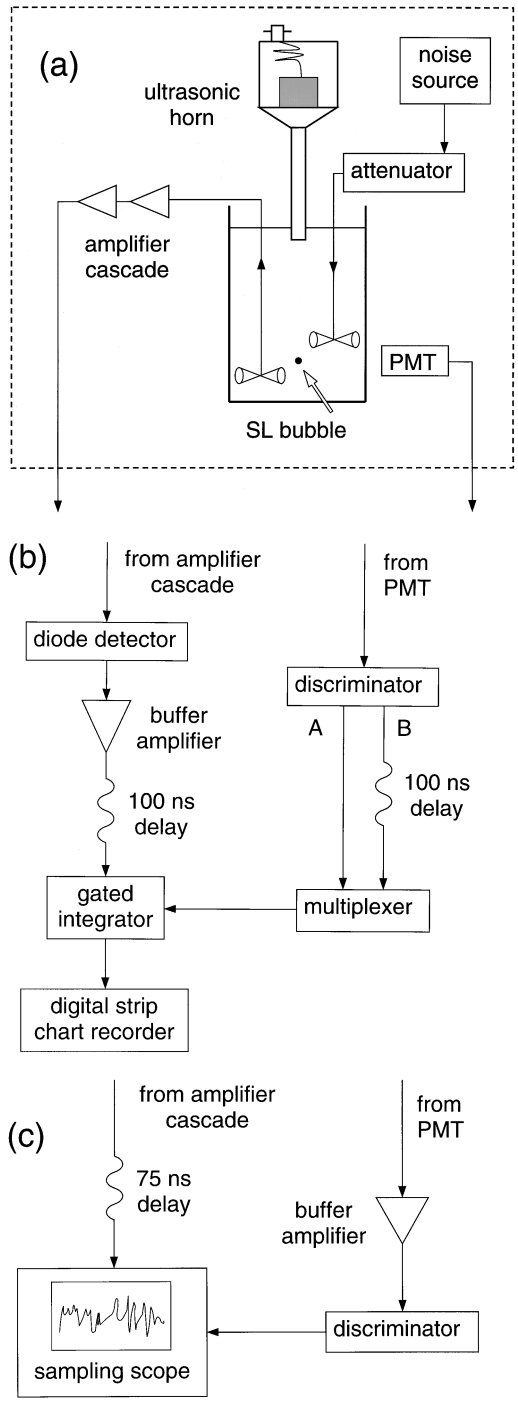

FIG. 2. Schematic diagrams of (a) a rectangular SL cell with driving horn and radiometer antenna, where the transmission antenna on the right is essentially identical to the receiver antenna on the left, and where the dashed line refers to a Faraday cage; (b) the arrangement for the gated integrator measurement; and (c) the arrangement for the sampling oscilloscope measurement.

The radiometer we built to measure microwave emissions consisted of a solid brass full-wavelength biconical dipole antenna [Fig. 2(a)] that was fed through a thin semirigid coaxial cable to a cascade of low-noise microwave amplifiers. The biconical geometry provides the flattest impedance response over the desired frequency range [9]. The antenna had a full length of 2.0 cm, with a 20° conical half-angle, and was positioned in the water approximately 2.0 cm from the bubble. The output of the first stage amplifier, which had a gain of 23 dB, was fed to an additional cascade of one or two amplifiers to provide an overall gain of 51 or 76 dB depending upon the method of detection (see below). Juxtaposed to the cell was a shielded photomultiplier tube (PMT), which provided a trigger to precisely identify the occurrence of a SL emission.

The above apparatus were housed in a Faraday cage made of 3-mm-thick aluminum sheets that were welded together. The cage had dimensions 60×90 cm^2, and height 60 cm. To prevent unwanted external microwave noise from entering the system, we sealed the access door with rf-shielded stripping, and secured the door with heavy spring-loaded latches. We also buffered the acoustical inputs to the cell with double rf-attenuating (''T'') filters.

The dominant source of noise in the system was the internal noise of the first stage amplifier. The noise power of an amplifier is given in terms of an effective noise temperature $T_{\rm eff}$ as $P=kT_{\rm eff}\Delta f$, where k is Boltzmann's constant and Δf is the bandwidth [10]. In our case the effective noise temperature was $T_{\rm eff}=120$ K and the bandwidth was $\Delta f=0.7$ GHz, which resulted in a front end noise power of $P=1.2$ pW. It is this noise power with which the received power coupled from the antenna competes. Additional amplifiers had a negligible contribution to the overall system noise because the effective noise temperatures add as $T_{\rm total}=T_1+T_2/G_1+T_3/G_1G_2+\cdots$, where T_n and G_n are the noise temperature and gain of the nth stage [10].

The amount of power coupled from the radiation field into the first-stage amplifier is a function of the antenna geometry and the impedance match of the antenna feed to the transmission line into the amplifier. The amount of power the antenna couples from the radiation far field is specified by the effective aperture area $A_{\rm em}$. The coupled power is $A_{\rm em}S$, where the magnitude of the Poynting vector is $S=e^{-\alpha r}P_{\rm bubble}/4\pi r^2$, where α is the attenuation coefficient, r is the distance from the bubble to the antenna, and $P_{\rm bubble}$ is the power that the bubble emits in the bandwidth of the amplifier cascade. The effective aperture in our case is calculated [11] to be $A_{\rm em}=4\lambda\pi^3$, where λ is the wavelength. The power coupled into the antenna is then

$$P_{\rm antenna}=e^{-\alpha r}\frac{4\lambda^2}{\pi^3}\frac{P_{\rm bubble}}{4\pi r^2}. \tag{1}$$

From Fig. 1, for $f=2.0$ GHz and room temperature, the attenuation coefficient is $\alpha=0.80$ cm^{-1}. For the distance $r=2.0$ cm from the bubble to the antenna, which is in the far field due to the smallness of the bubble [11], and for the wavelength $\lambda=1.7$ cm, Eq. (1) yields a received power efficiency of $P_{\rm antenna}/P_{\rm bubble}=1.5\times10^{-3}$. This is further reduced by a polarization loss of $\frac{1}{2}$, as well as an impedance mismatch efficiency between the antenna and first-stage amplifier, which was determined to be 0.30 from the value of the reflection coefficient directly measured with a network analyzer. The power efficiency into the amplifier cascade is then $P_{\rm feed}/P_{\rm bubble}=2.2\times10^{-4}$.

Two alternative methods were employed to measure the signal from the amplifier cascade. In the first method [Fig. 2(b)], the signal from the amplifier cascade with gain 76 dB was fed to a tunnel diode detector whose output was buffered

through a high impedance amplifier and sent through a delay of approximately 100 ns into a gated integrator. The gated integrator was triggered as follows. The output of the PMT was sent into a discriminator module. In order to difference the SL signal from the background, we employed two outputs *A* and *B* from the discriminator module, where *B* was delayed 100 ns relative to *A*. The timing of *A* was such that the gated integrator was triggered 5 ns before the buffered diode signal arrived. The baseline subtract feature of the gated integrator was employed. In this mode of operation the gated integrator, when triggered by *A*, would integrate for 20 ns during which a SL signal was present. On the next acoustical cycle the gated integrator was triggered by *B*, and the integration window was delayed 100 ns after the SL signal had passed. This baseline value was subtracted from the previous value of the signal plus baseline, and the result was forwarded to an exponential summer whose output was recorded on digital strip chart (Stanford Research Systems model 850 lock-in amplifier). Averaging over roughly 2.0×10^3 s was then performed to yield the ultimate sensitivity.

In the second method [Fig. 2(c)] to measure the microwave power, we employed a sampling oscilloscope with picosecond resolution (Hewlett-Packard model 54750A high-bandwidth digitizing oscilloscope) to sample the microwave signal repetitively directly from the amplifier cascade. The voltage of the signal was measured once per SL flash with respect to a stable trigger, where the sample time was successively incremented relative to the trigger time. Because this technique allows only one sample to be made for each trigger, the result does not allow a direct temporal series wave form to be created of any particular SL flash. However, this limitation is of no consequence here, because the microwave signal is a noise fluctuation and not a repetitive wave form. In order to provide a stable trigger to the digitizer, the buffered output from the PMT was used. The microwave signal was sent through a 75-ns delay in order to allow for the internal delay of the sampling oscilloscope (22 ns) and the collective delay of the buffer amplifier and discriminator (52 ns). For this arrangement, the amplifier cascade had a gain of 51 dB rather than 76 dB, in order to avoid overloading the input of the sampling oscilloscope.

A pulsed noise system [Fig. 2(a)] was used to calibrate the sensitivity of the radiometer. The system contained a microwave noise source and a fast microwave diode switch, and was housed in a small aluminum enclosure inside the Faraday cage. The source consisted of two cascaded amplifiers with the input of the first grounded. The output was fed into the switch and then passed through the aluminum enclosure to a biconical dipole transmission antenna which was identical to the receiver antenna described above. The transmission antenna was placed inside the cell opposite the receiver antenna. The noise switch was normally in the off position, which provided 30 dB of attenuation between the transmission antenna and the noise source. The amount of noise power transmitted from this source was controlled by placing a series of attenuators between the output of the enclosure and the feed of the transmission antenna. The switch was activated by a short negative pulse of approximate duration 8 ns from a fast pulse generator. To trigger the PMT, this pulse also fired a light-emitting diode that was mounted to the top of the aluminum enclosure. Because the diode detector had a relatively long relaxation time, there was a negligible difference in the output voltage when it was activated by the 8-ns calibration noise pulse or the 50–380-ps SL pulse.

We determined the minimum detectable power of the system as follows. With the diode detector and the gated integrator (first method described above), the power of the cali-

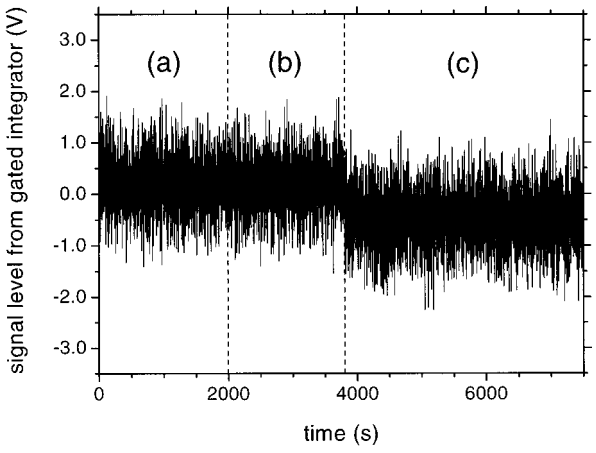

FIG. 3. Gated-integrator output of the SL microwave radiometer with a xenon-doped bubble: (a) SL on, (b) ambient reading with SL off, and (c) calibration noise source on. The noise shifts the average output negative. The calibration noise power corresponds to 3.0 times the minimum value established by averaging.

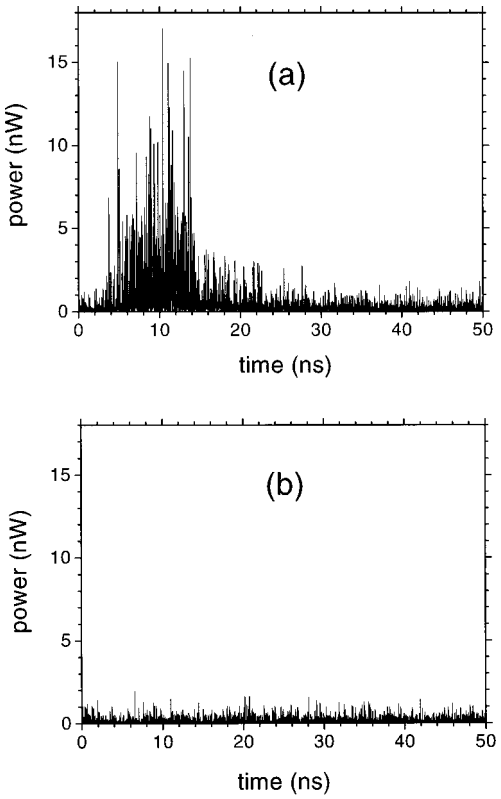

FIG. 4. Data with the sampling oscilloscope: (a) calibration noise source, which corresponds to 3.0 times the minimum detectable power; and (b) data for SL emission from a xenon-doped bubble, which show no signal in the ambient noise on a time scale of 50 ps or more.

brating noise was increased from zero until this noise just became apparent in the ambient noise. Figure 3(c) shows noise calibration data corresponding to 3.0 times the minimum detectable power. We set an upper limit on the corresponding amount of microwave power radiated into the cell by measuring the output power at the noise source with a calibrated power meter with the noise source held on continuously, and then accounting for the attenuators. The amount of power the radiometer received was measured in a similar fashion by connecting the power meter directly to the output of the amplifier cascade with the noise source again held on continuously, and with a series of attenuators between the noise source and the calibration antenna. The radiated power of the calibrating transmission antenna had a duration of 8 ns at a power level of 2 nW in the bandwidth of the detector. This set a minimum detectable power received by the antenna to be approximately $P_{\text{antenna}}=2.0$ pW. By comparison, this minimum detectable power is three orders of magnitude greater than that of COBE (Cosmic Background Explorer) after extensive and sophisticated data processing techniques were employed [12]. From Eq. (1), the corresponding upper limit to the minimum detectable power of the bubble was $P_{\text{bubble}}=1.3$ nW, which corresponds to approximately 10^5 photons for a 100-ps emission time, and to roughly one photon emission per gas atom in the bubble per SL flash.

The minimum detectable power of the bubble for the sampling oscilloscope measurement method was 20 nW. Figure 4(a) shows noise calibration data corresponding to 3.0 times the minimum detectable power. The radiated power of the calibrating transmission antenna had a duration of 8 ns at a power level of 6 nW in the bandwidth of the detector. Figure 4(a) shows the average of four samples taken with the noise source on, and differenced from a sample taken with the noise source off. It is clear from this figure that a resolution of less than 1 ns is possible.

Results obtained from both air and 2% xenon-doped bubbles with the gated integrator measurement method show no evidence of microwave emission at or above the minimum detectable power of $P_{\text{bubble}}=1.3$ nW. Xenon was used because it is observed to yield the greatest optical emission, exceeding the emission of an air bubble by a factor of 10. Figure 3 shows the results of a gated integrator measurement. The average voltage of the signal for xenon with the SL present was 0.203 ± 0.388 V, and the average with no SL was 0.178 ± 0.380 V, while the average with a transmitted noise pulse at 3.0 times the minimum sensitivity was -0.471 ± 0.397 V. Figure 4(b) shows results of a sampling oscilloscope measurement for a xenon-doped SL bubble. The measurements made with the sampling oscilloscope show no evidence of microwave emission at or above the minimum detectable power of $P_{\text{bubble}}=20$ nW.

The quest to understand sonoluminescence is not limited to emission in the visible and near-visible regions, but extends to the entire electromagnetic spectrum. Due to the absorptive properties of water, it is natural also to consider the microwave region. We have experimentally established an upper limit of the microwave power radiating by a bubble to be 1.3 nW in a 0.7-GHz band centered at 2.0 GHz. Any emission theory must be consistent with this observation.

We are grateful for discussions with Bradley Barber, Felipe Gaitan, Paul Goggins, Robert Hiller, Keith Weninger, Andrés Larraza, Seth Putterman, and Charles Smith. We are also grateful to Hewlett-Packard for their loan of the high-bandwidth digitizing oscilloscope (Model No. 54750A). This work was supported in part by a grant from the U.S. Office of Naval Research.

[1] C. C. Wu and P. H. Roberts, Proc. R. Soc. London, Ser. A **445**, 323 (1994).
[2] Robert Hiller, Seth J. Putterman, and Bradley P. Barber, Phys. Rev. Lett. **69**, 1182 (1992).
[3] Julian Schwinger, Proc. Natl. Acad. Sci. USA **90**, 2105 (1993).
[4] Claudia Eberlein, Phys. Rev. A **53**, 2772 (1996).
[5] Lothar Frommhold and Anthony A. Atchley, Phys. Rev. Lett. **73**, 2883 (1994).
[6] J. D. Jackson, *Classical Electrodynamics*, 2nd ed. (Wiley, New York, 1974), pp. 290–292.
[7] *Water: A Comprehensive Treatise. Vol. 1, The Physics and Physical Chemistry of Water*, edited by Felix Franks (Plenum, New York, 1972), pp. 277–287.
[8] F. B. Seeley and C. K. Joens, Am. J. Phys. **66**, 259 (1998).
[9] George H. Brown and O. M. Woodward, Jr., RCA Rev. **13**, 425 (1952).
[10] G. Evans and C. W. McLeish, *RF Radiometer Handbook* (Artech, Dedham, MA, 1977).
[11] Constantine A. Balanis, *Antenna Theory Analysis and Design* (Harper and Row, New York, 1982), pp. 112–132.
[12] Barbara G. Levi, Phys. Today **45** (6), 17 (1992); G. Smoot *et al.*, Astrophys. J. **360**, 685 (1990).